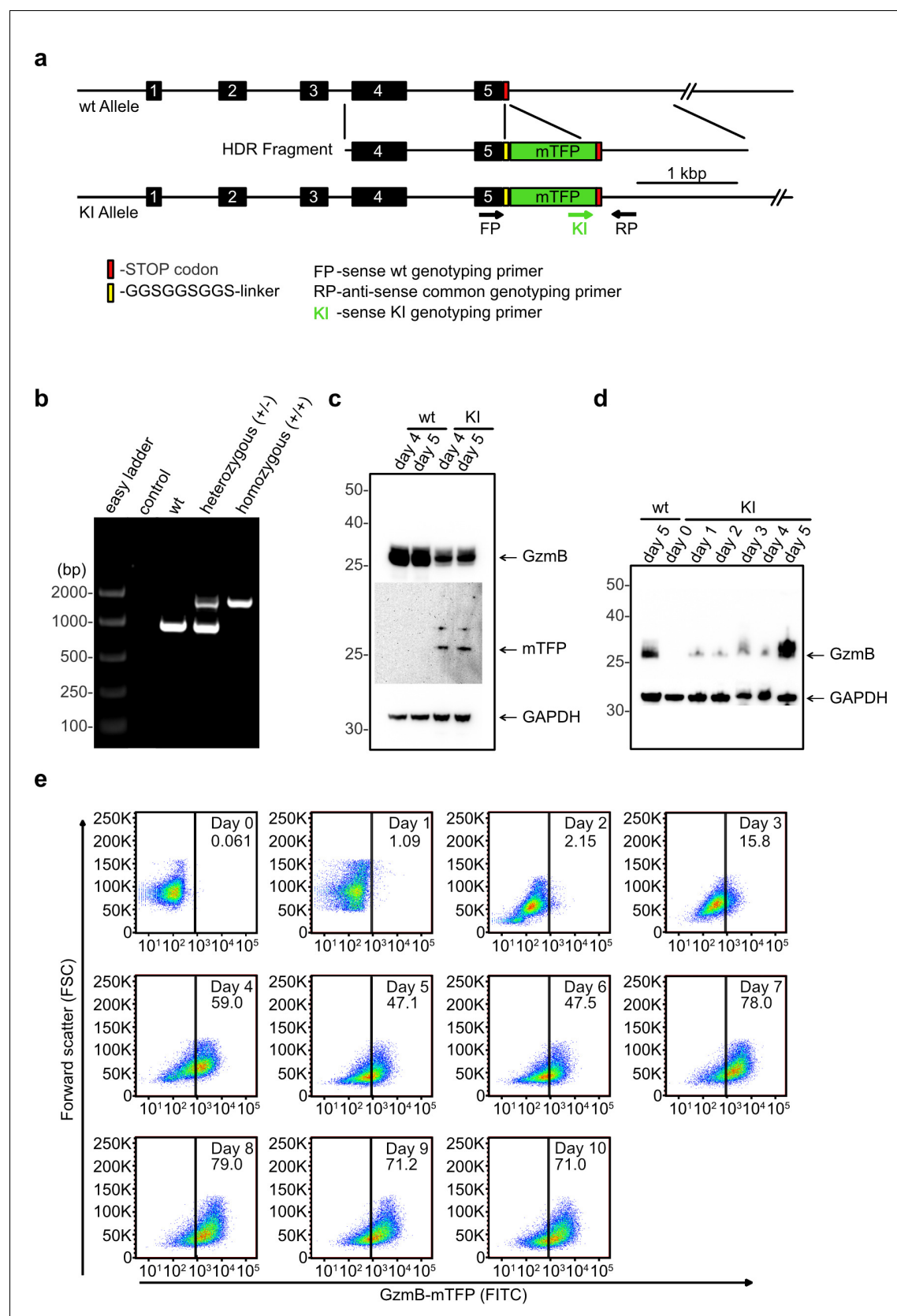


---

## Figures and figure supplements

Studying the biology of cytotoxic T lymphocytes in vivo with a fluorescent granzyme B-mTFP knock-in mouse

**Praneeth Chitirala et al**



**Figure 1.** Generation of GzmB-mTFP knock-in mice. (A) CRISPR-Cas9 strategy to generate the GzmB-mTFP-KI. wt, wild-type; KI, GzmB-mTFP-KI; numbered black boxes, *Gzmb* exons; red bar, Stop codon; yellow bar, GGSGSGGS-linker; green box, mTFP coding sequence; rightward black arrow, Figure 1 continued on next page

*Figure 1 continued*

forward genotyping primer wt; rightward green arrow, forward genotyping primer KI; leftward black arrow, reverse common genotyping primer (primers are not drawn to scale). **(B)** PCR of CTL lysates derived from wild-type, heterozygous and homozygous GzmB-mTFP-KI mice using oligonucleotides FP, RP and KI. **(C)** Western blot of lysates derived from wild-type and GzmB-mTFP-KI CTLs 4 and 5 days after activation. Anti-GzmB and anti-mTFP antibodies were used for detection, anti-GAPDH antibody served as loading control. **(D)** Western blot of lysates derived from naïve GzmB-mTFP-KI CTLs and 1, 2, 3, 4 and 5 days after activation with anti-CD3/anti-CD28 coated beads. Lysates from wild-type CTLs 5 days after activation were used for comparison, anti-GAPDH antibody served as loading control. **(E)** CTLs from GzmB-mTFP-KI mice were isolated and analyzed by FACS at the indicated days after activation. Non-activated CTLs (day 0) served as negative control.

```

GCCCCCTCTTGCTCTCATCTCTCAATTTCTCCCTTTTCATCCTGGCCTTCATGGTGTTCAGACCAGCAGGCCATGAGCT      80
GGACTCTTGCTTCTTCCCAACAGCTGAAGAGTAAGGCCAAGAGGACTAGAGCTGTGAGGCCCTCAACCTGCCAGGCG      160
CAATGTCAATGTGAAGCCAGGAGATGTGTGCTATGTGGCTGGTTGGGGAAGGATGGCCCCAATGGGCAAATACTCAAACA      240
CGCTACAAGAGGTTGAGCTGACAGTACAGAAGGATCGGGAGTGTGAGTCTTCTTAAAAATCGTTACAACAAAACCAAT      320
CAGATATGTGCGGGGGACCCAAAGACCAAACGTGCTTCCCTTTCGGGTAAGTTGGGTGCAGTCCCCCTCTGGGCTAAGTGG      400
GAGGGGAAAAGGAATCTGGGACCTAGAGACCCAAATATCAAGGACTCCTTTACCCACTGGCTGTGATCTTCTCCCTGG      480
GAACAGCAGGTACTAGTAATGAAGTGGGGCCCCCAGAGCTGACTAGGAGCCTCTGCTGAAGGTAGCTTGTACAAAAGGAG      560
GTGTTGGCAACACAGTACCTGTCCCAGGCCAGGCTGTAGAAAGCTGGGCTCCCTGGGTGTGTCATAACCACACCCATGT      640
GTCTCCTCTGAGCAGACACACACTTTGTCTAGTGGGCTTCCCTCCATGCTCACACCTGGCCCCACTCACTGTCCCCATGTC      720
CTTAAACAACAGCCTAGAGACGAGGGTCCACACACCTTCTTAGAGCGTGGATCACAGACCTGGGGAAAAGGGCAGAGGCT      800
GCCTCAGGAGGGAGGTGCAGCCCTAACCATGTCCACAGTCAAGAGCTGGGAAGGCCGGGGGGCCCCAGGACTGTCTCTGAC      880
CTCCCATAGCATAAATCATGCTTCTCTGGGAGGAGCCTTGACATGAGGAGGTGGGACCAGGGTGAAACAACAGCTCAGT      960
GCCTTGTATCCACTCAATTCACAGGGGGATTCTGGAGGCCCGCTTGTGTGTAAAAAAGTGGCTGCAGGCATAGTTTCCTA      1040
TGGATATAAGGATGGTTACCTCCACGTGCTTTCACCAAAGTCTCGAGTTTCTTATCTGGATAAAGAAAAAATGAAAA      1120
GCAGCGGGAGCGCGGGAAGCGCGGTACCATGGTGAGCAAGGGCGAGGAGACCACAATGGGCGTAATCAAGCCGAC      1200
ATGAAGATCAAGCTGAAGATGGAGGCAACGTGAATGGCCACGCCTTCGTGATCGAGGGCGAGGGCGAGGGCAAGCCCTA      1280
CGACGGCACCAACACCATCAACCTGGAGGTGAAGGAGGGAGCCCCCTGCCCTTCTCTACGACATTCTGACCACCGCGT      1360
TCGCCTACGGCAACAGGGCCTTACCAAGTACCCGACGACATCCCCAACTACTTCAAGCAGTCTTCCCCGAGGGCTAC      1440
TCTTGGGAGCGCACCATGACCTTCGAGGACAAGGGCATCGTGAAGGTGAAGTCCGACATCTCCATGGAGGAGGACTCCTT      1520
CATCTACGAGATACACCTCAAGGGCGAGAACTTCCCCCCCCAAGGCCCGGTGATGCAGAAGAAGACCACCGGCTGGGACG      1600
CCTCCACCGAGAGGATGTACGTGCGCGACGGCGTGTGAAGGGCGACGTCAAGCACAAGCTGCTGCTGGAGGGCGGGCGG      1680
CACCACCGCGTTGACTTCAAGACCATCTACAGGGCCAAGAAGGCGGTGAAGCTGCCGACTATCACTTTGTGGACCACCG      1760
CATCGAGATCTCGAACCAGCACAAGGACTACAACAAGGTGACCGTTTACGAGAGCGCGGTGGCCCGCAACTCCACCGACG      1840
GCATGGACGAGCTGTACAAGTAACTACAGAAGCAACATGGATCTGCTGTGTTAGCCATCGTCCCTAGAGCTGAGTCCA      1920
GATTGCTGTACGACAGTGGCAGGATCTGAATAAAGGACTGCAAAGACTGGCTTCATGTCCAATTCACAAGGACCAGCTC      2000
TGTCTTGGCAGGCCAATGGAACACCTCTTCTGCCACCATGCTGTGACAACCCAACTGACATCTTCCATGGAAGTTTGC      2080
CCTCTCCACAAAAGAAGTAGAATGTTTGCATTGGAGCTGGGCATGCTCTGCTTCCCTCAGTGCCCCGAGAATGTTATCT      2160
AATGCTAGTCAATTAATAGCTCCCTACAGAACTTTCATACAGTTGCACCCAAAGTTGCTGATGTGTTCTCTAGAATAGA      2240
GCAAGAAATAGTAAACAGAATTCCTTTTGCCTCTCTGTACTATTTTCCCCCAAATACCAAGATTTGTATGTTTTATAAAG      2320
CTAATTTCTTATCAAATGACATCTTTTAATTTTACATTAATGGCTTATTTTCAAGGTACAACCTGATTTTTTTATGGA      2400
CAAAAATGATGTAAAATCAAATAAACTAATTAATATATCCATTAATTTAAATACTTTTATTTTGAAGGGAAGTCATA      2480
AGTATGTTTGTAGAAATTTTGAATGTACAAGGTACTATTAGTTAATAGTTATGCAGTAGGCTTCAAAAAGTGATTCAT      2560
GCCCTCTAATTGAAATTTCTGTAGTCTTTGATCAATATTTTCCATTTCTAATCTGCCAGCCTCCAGTAACCACTATTCTC      2640
TCTACTTCTACAAATTTCCATTGTTTATAGATTTTAAACACAAGTAAGATCATGCATTTTTTTTCTAGTATGCCTAGATTAT      2720
TTGGCTTGGAAATCATGTCTCAGTGCAAGTCTATCATTTGTAAGAGTAGAATTTTATCATCTTAATGCCTGGATAATGAG      2800
ATAAAGAGATGGCTCAACAGTTTATAGCACTTTAACAGAGGACTCAGGTTCAATGGCCAGAATACACATTATGTATGTCT      2880
CACAACCATCTTTACTCCAACCTCCAGGGCAACACACACACACACACACACACACACACACACACACACACACACACC      2960
ATGTACAAATATTTCCACACATACATAAATACAATTTTAAATTTAATATCTTATGCATGTGCCACATTGTCTCTATGCT      3040
CCCATTCTATTGATGAAGATGGGTCAACCTTTAGCTGTTGGGAATATTGTTACAATAAGCATGAGAGTATAGATGTAGGGG      3120
ACCTGGGAAAGCATACCCAGACACCAAGTTCTCCATACAAAGGAGACTTATTACCAAGACAGACAAGTAGGTTTGGCGT      3200
CAGGGAGGTGACTGCCTTTGTATTGGAT      3228

```

Sense WT Genotyping Primer	<u>BLACK UNDERLINED</u>
Sense KI Genotyping Primer	<u>RED BOLD UNDERLINED</u>
Antisense Common Genotyping Primer	<u>BLACK ITALIC UNDERLINED</u>
Exons 4 and 5	<b>BLACK BOLD</b>
GGSGGSGGS-Linker Coding Sequence	<b>BLUE BOLD</b>
mTFP Coding Sequence	<b>RED BOLD</b>
STOP Codon	<b>TAA</b>
Introduced Mutations	<b>GREEN BOLD</b>

**Figure 1—figure supplement 1.** Design of the HDR fragment to generate the GzmB-mTFP-KI. The HDR fragment was designed to replace the endogenous Stop codon of the *Gzmb* gene by sequences encoding a GGSGGSGGS-linker, mTFP and a Stop codon. Some sites were mutated (green). *Figure 1—figure supplement 1 continued on next page*

*Figure 1—figure supplement 1 continued*

bold) to protect the HDR fragment against cleavage in the presence of the sgRNA used, and of sgRNAs that had initially been envisioned for this project but were ultimately not used. The proper insertion of the HDR fragment into the genome was determined by PCR. For this purpose, we used primer 36016 (5'-ATC AAA GAA CAG GAG AAG ACC CAG-3', Exon 3) in combination with primer 33615 (5'-GGT GTT GGT GCC GTC GTA GGG-3', mTFP) (1433 bp fragment) and primer 19524 (5'-ACC GCA TCG AGA TCC TGA ACC-3', mTFP) in combination with primer 36017 (5'-AAT GGC TAA GCA ATC CCA TCA GG-3', downstream of HDR1) (1565 bp fragment).

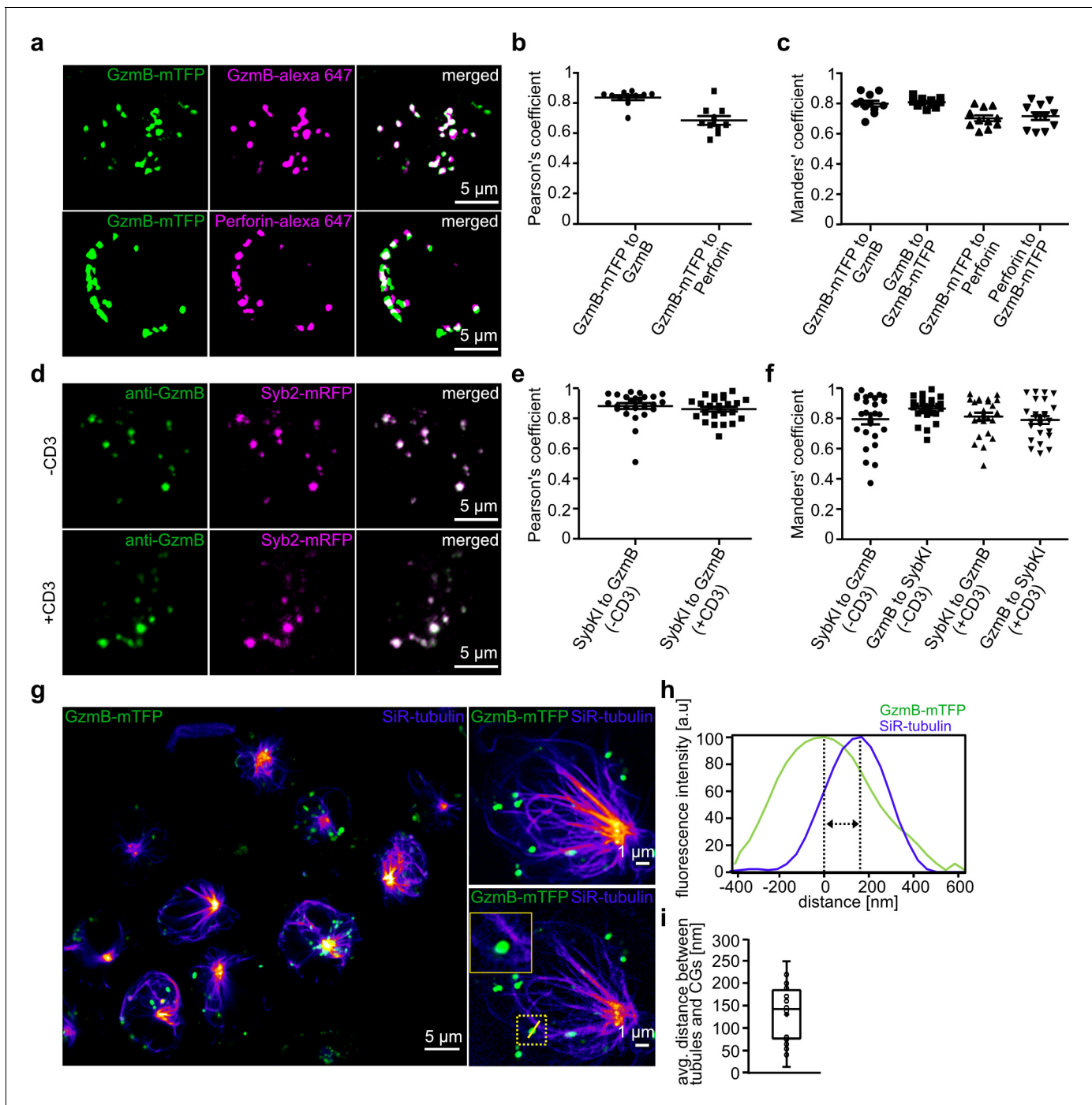


**Figure 2.** Endogenous GzmB-mTFP fluorescence co-localizes with CG markers and migrates to the IS. (A) SIM images of primary CTLs from GzmB-mTFP-KI mice on day five after activation. CTLs were fixed and stained with Alexa647 conjugated anti-GzmB antibody (upper panel) or Alexa647 conjugated anti-perforin antibody (lower panel). (B–C) Pearson's and Manders coefficients of correlation between GzmB-mTFP and the other CG markers. (D) SIM images of primary CTLs from Syb2-mRFP/GzmB-mTFP double KI mice on day five after activation. CTLs were fixed and examined for endogenous fluorescence in the mTFP and mRFP channels. (E–F) Pearson's and Manders coefficients of correlation between GzmB-mTFP and Syb2-mRFP. Scale bars, 5  $\mu$ m. (G) Live STED images of primary CTLs from GzmB-mTFP-KI mice labeled with SiR-tubulin and plated onto anti-CD3 coated coverslip. The transport of CG along the microtubules toward the IS is shown in the overview for all CTLs (left; Scale bar, 5  $\mu$ m) and in more detail in the two exemplary CTLs (right; Scale bar, 1  $\mu$ m). (H) Distance between CG and microtubule from exemplary image quantified by ImageJ software. (I) Average distance between microtubules and CGs (n = 19).

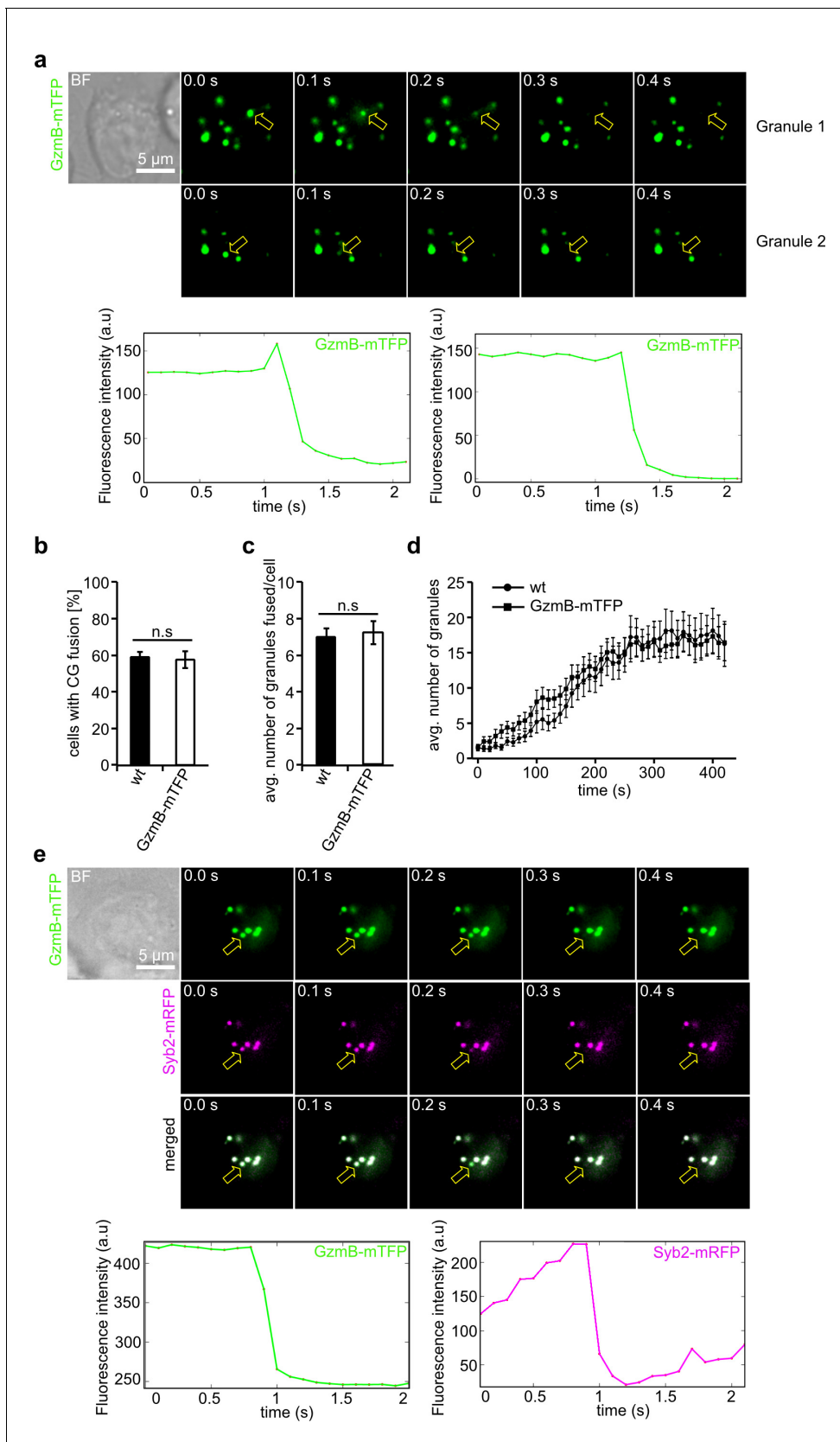


**Figure 3.** GzmB-mTFP containing cytotoxic granules fuse at the IS. (A) Selected live-cell TIRF microscopy images of GzmB-mTFP in a CTL in contact with an anti-CD3 coated coverslip. Fusion events are indicated with open arrows (seven consecutive frames per fusion event are shown). Scale bar, 5  $\mu$ m. Figure 3 continued on next page

*Figure 3 continued*

$\mu\text{m}$ . **(B)** Selected live-cell, dual-channel TIRF microscopy images of GzmB-mTFP and Syb2-mRFP in a CTL derived from Syb2-mRFP/GzmB-mTFP double KI mice and in contact with an anti-CD3 coated coverslip. Fusion events are indicated with open arrows (seven consecutive frames per fusion event are shown). **(C–D)** Comparison between wild-type and GzmB-mTFP-KI CTLs reveals no difference in the percentage of CTLs showing fusion **(C)** and average number of fused CG per cell **(D)**. **(E)** Mean average number of CGs appearing in the TIRF plane per cell during 7 min of measurements ( $N = 3$ ,  $n = 10$  for wt; and  $N = 3$ ,  $n = 12$  for GzmB-mTFP KI).



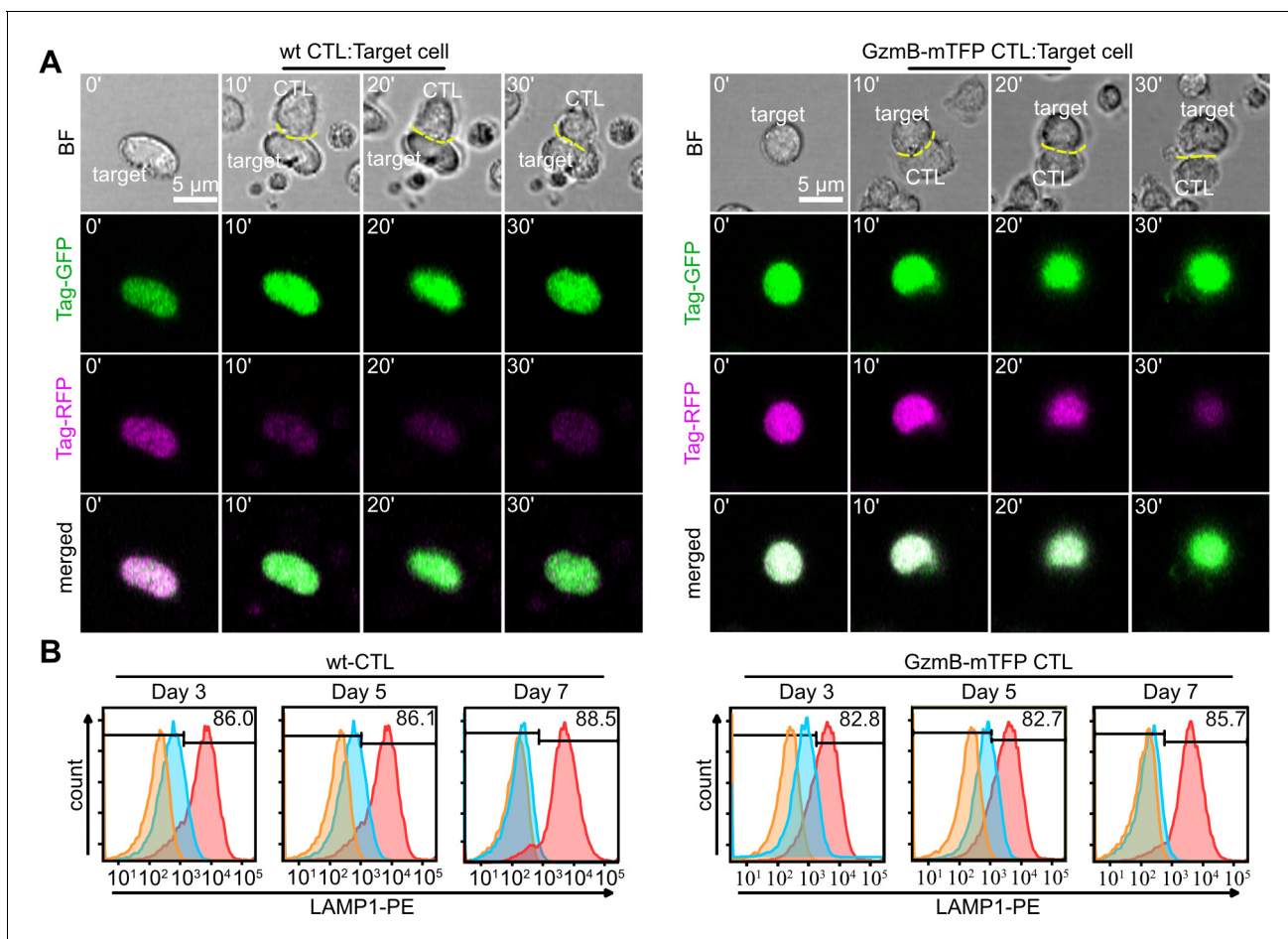


**Figure 4.** CTLs from GzmB-mTFP-KI mice kill target cells as efficiently as wild-type CTLs. **(A)** Live cell killing assay showing a wild-type (left) and GzmB-mTFP-KI (right) CTL in contact with P815 target cells stably expressing Casper3-GR (FRET construct containing Tag-GFP and Tag-RFP with a target cleavage site DEVD of Caspase 3 (activated via GzmB). LSM images at indicated time points show a reduction in FRET signal, indicating the killing of the target cell. Scale bars, 5  $\mu$ m. **(B)** CTLs isolated from either wt (left) or GzmB-mTFP-KI (right) mice were assessed for degranulation capacity using FACS-based assay on day 3, 5 and 7, respectively. Data shown are representative histograms from three independent experiments. Orange areas show untreated CTLs, blue areas show constitutive secretion and red areas show stimulated secretion.

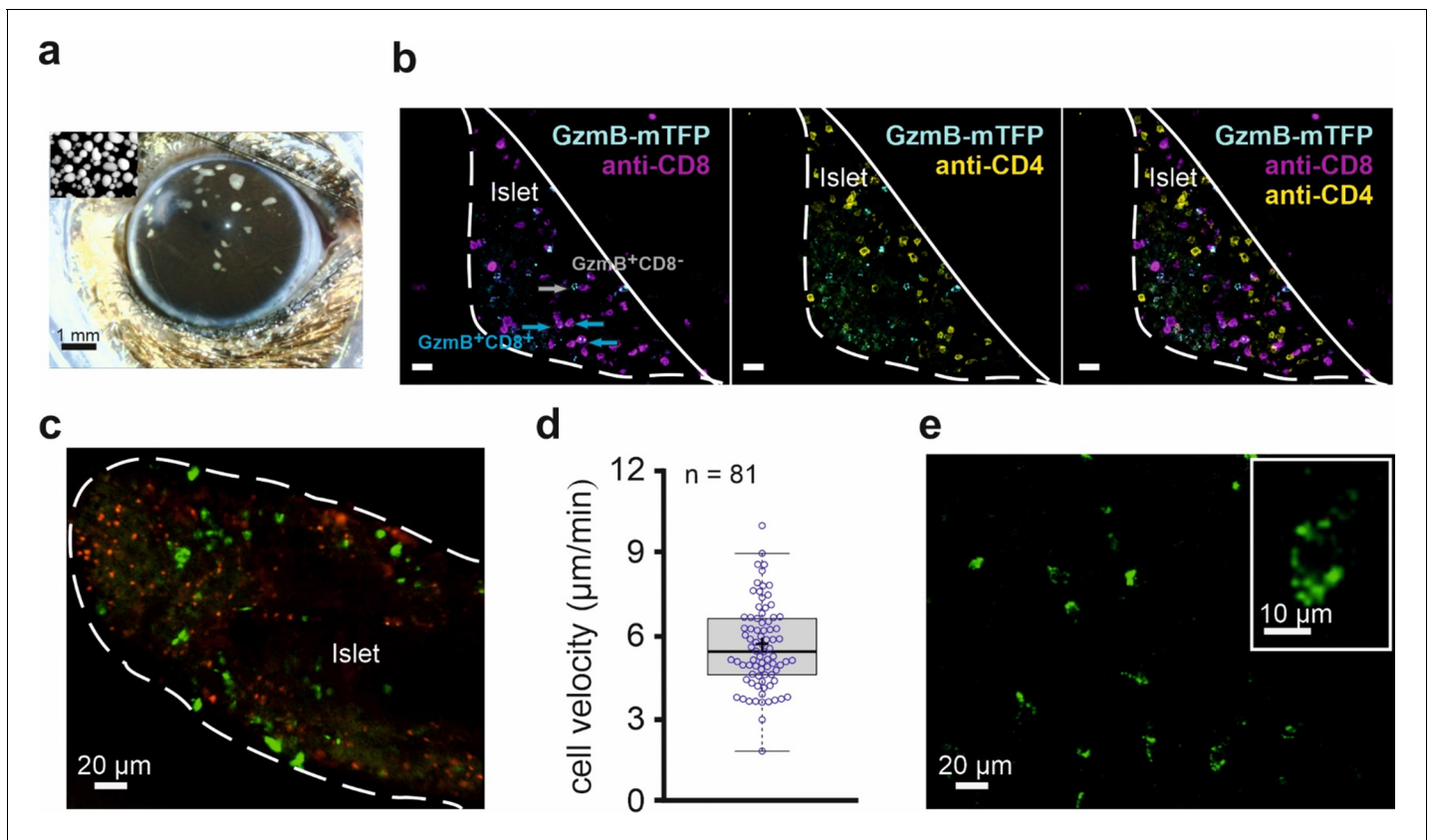


**Figure 5.** In vivo imaging of allorecjection in the anterior chamber of the eye (ACE) visualized by CTLs from GzmB-TFP-KI mice. **(A)** Binocular image of a mouse eye with islets of Langerhans from DBA/2 mice transplanted into the anterior chamber of the eye (ACE) 4 days prior to the image. Islets can be identified as small white spots in the range between 100–300  $\mu\text{m}$  diameter located on top of the iris. Inset shows cultured islets before transplantation. **(B)** Confocal images of a pancreatic islet inside the ACE fixed and sliced at POD14. The outline defines the boundary of the islet of Langerhans localized on the iris. Green cells are cytotoxic T lymphocytes marked by endogenously expressed GzmB-mTFP having infiltrated the islet during the immune response. Antibody staining of CD8<sup>+</sup> (blue) and CD4<sup>+</sup> (magenta) T cells are shown. **(C)** In vivo confocal microscopy of an islet during allorecjection in the ACE (POD14). White line marks the boundary of pancreatic islet toward the ACE lumen. Faint green (excitation 458 nm wavelength) and red (excitation 561 nm wavelength) signals are autofluorescence. CTLs marked by GzmB-mTFP (green, excitation 488 nm) infiltrated the islet during the immune response. **(D)** Velocity of 81 migrating CTLs tracked from panel (C) after imaging for >30 min. Mean is shown as a plus symbol, median as a line. See also **Figure 5—video 1**. **(E)** Two-photon image of GzmB-mTFP positive cells from the corneal area. Individual vesicles inside the CTL are easily identified (inset). See also **Figure 5—video 2**.

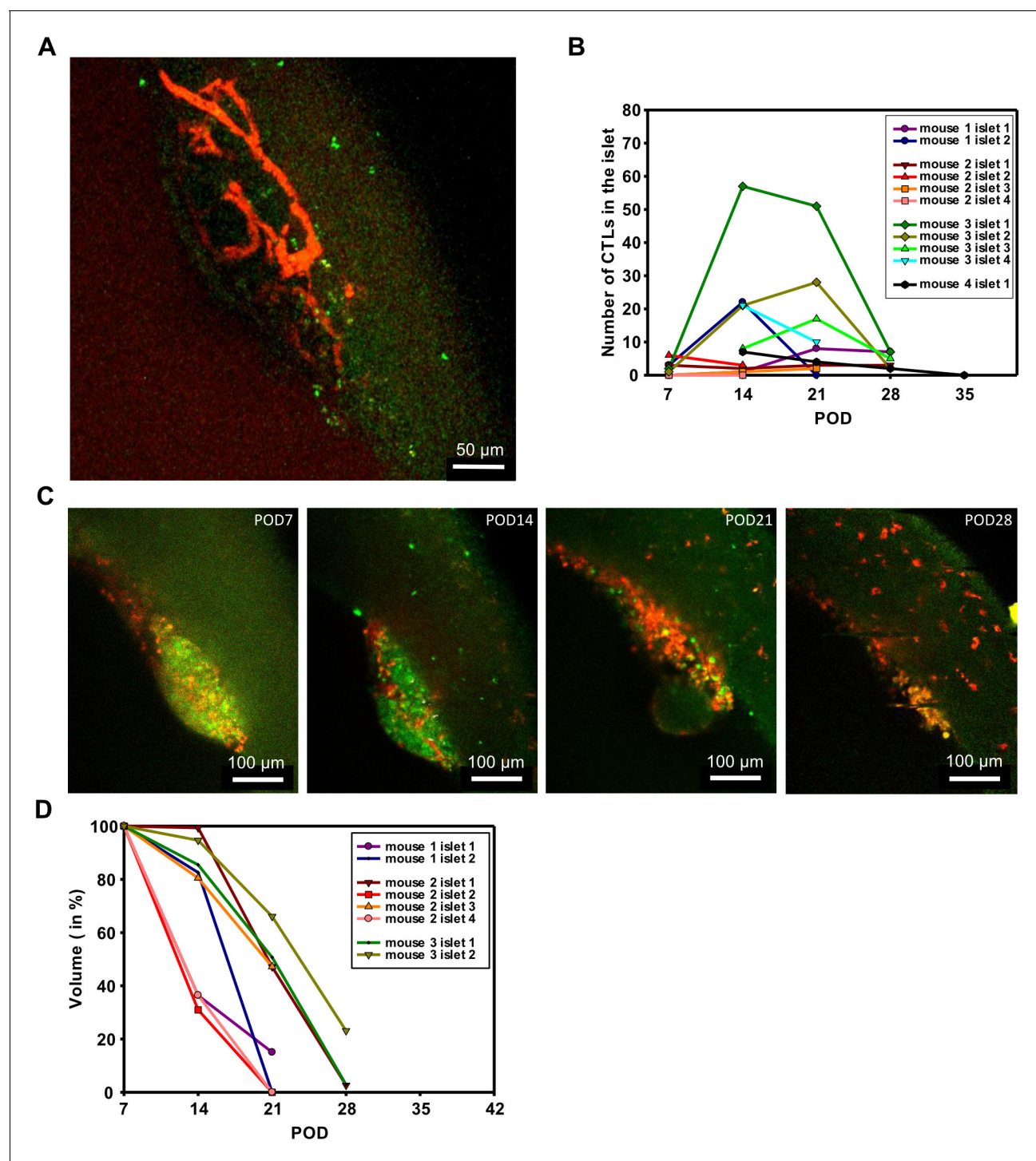


**Figure 5—figure supplement 1.** Longitudinal and repetitive observations of transplanted islets inside the ACE. **(A)** Two-photon image at POD14 of the capillary network of a transplanted islet. Rhodamine-dextran was injected into the tail vein of the mouse 15 min before acquisition to label blood vessels. Vessels are displayed in red and GzmB-mTFP positive cells in green. For excitation the two-photon laser was tuned to 880 nm for GzmB-mTFP and 1040 nm for rhodamine-dextran. A video of the imaged islet is shown in **Video 1**. **(B)** Quantitative analysis of the number of CTLs (GzmB-mTFP positive cells) approaching the islets are displayed as a function of time. Data from 11 islets from four different animals are shown. Each animal was in vivo imaged repetitively over 4 to 5 weeks (POD7-35). **(C)** Series of weekly acquired confocal in vivo images of the same islet demonstrating tissue rejection. Images show maximum intensity projections of a 40  $\mu\text{m}$  thick stack (11 planes) through a group of islets. Brightness of the image is heavily stretched to visualize islets by faint autofluorescence. Scale bars: 100  $\mu\text{m}$ . **(D)** Reduction of islet volume during rejection. Stacks of islets were acquired weekly and the volume was measured in 3D by surface rendering with Imaris software. Islet volume starts to shrink at POD14, at POD28 islets were completely rejected.